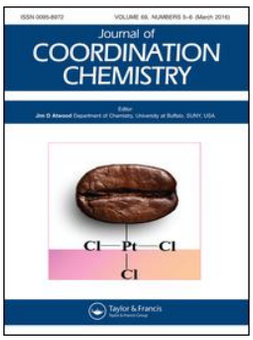

Journal of Coordination Chemistry

ISSN: 0095-8972 (Print) 1029-0389 (Online) Journal homepage: http://www.tandfonline.com/loi/gcoo20

Crystal structure and spectroscopic behavior of three new tris-oxalatoferrate(III) salts

Oscar E. Piro, Gustavo A. Echeverría, Roberto C. Mercader, Ana C. González-Baró & Enrique J. Baran

To cite this article: Oscar E. Piro, Gustavo A. Echeverría, Roberto C. Mercader, Ana C. González-Baró & Enrique J. Baran (2016) Crystal structure and spectroscopic behavior of three new tris-oxalatoferrate(III) salts, Journal of Coordination Chemistry, 69:24, 3715-3725, DOI: 10.1080/00958972.2016.1244670

To link to this article: http://dx.doi.org/10.1080/00958972.2016.1244670

Accepted author version posted online: 07 Oct 2016.
Published online: 17 Oct 2016.

JOURNAL OF COORDINATION CHEMISTRY, 2016
VOL. 69, NO. 24, 3715–3725
http://dx.doi.org/10.1080/00958972.2016.1244670

Taylor & Francis
Taylor & Francis Group

Crystal structure and spectroscopic behavior of three new *tris*-oxalatoferrate(III) salts

Oscar E. Piro[a], Gustavo A. Echeverría[a], Roberto C. Mercader[a], Ana C. González-Baró[b] and Enrique J. Baran[b]

[a]Facultad de Ciencias Exactas, Departamento de Física, Instituto Física de La Plata (IFLP, CONICET, CCT-La Plata), Universidad Nacional de La Plata, La Plata, Argentina; [b]Facultad de Ciencias Exactas, Centro de Química Inorgánica (CEQUINOR, CONICET/UNLP), Universidad Nacional de La Plata, La Plata, Argentina

ABSTRACT

A new general synthetic procedure for preparation of $Na_3[Fe(C_2O_4)_3]\cdot 5H_2O$ (**1**), $Rb_3[Fe(C_2O_4)_3]\cdot 3H_2O$ (**2**), and $Cs_3[Fe(C_2O_4)_3]\cdot 2H_2O$ (**3**) was developed. The crystal structures of these salts have been determined by single crystal X-ray diffraction. Salt **1** crystallizes in the monoclinic space group C2/*c* with $Z = 8$, salt **2** in $P2_1/c$ with $Z = 4$, and salt **3** in $P2_1/n$ with $Z = 4$. The three new salts and $K_3[Fe(C_2O_4)_3]\cdot 3H_2O$, prepared for comparative purposes, were further characterized by infrared and ^{57}Fe-Mössbauer spectroscopy. These spectra are discussed in comparison with those of related oxalato complexes.

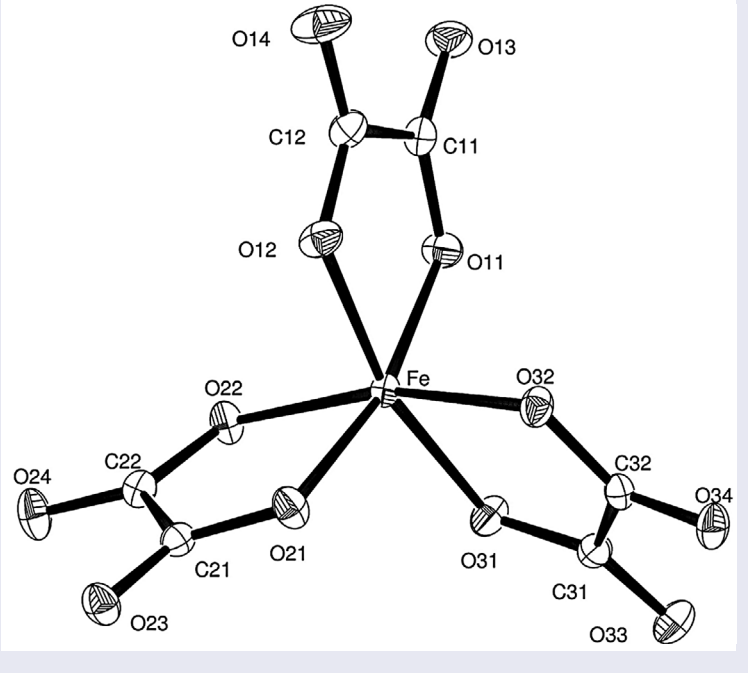

ARTICLE HISTORY
Received 10 May 2016
Accepted 24 August 2016

KEYWORDS
Tris-oxalatoferrate(III); alkaline salts; crystal structures; infrared spectra; ^{57}Fe-Mössbauer spectra

CONTACT Enrique J. Baran baran@quimica.unlp.edu.ar

1. Introduction

We have investigated the general physicochemical properties of numerous natural oxalates as well as their synthetic counterparts (for a recent review cf [1]). One particularly interesting natural oxalate mineral is minguzzite [1, 2], which synthetic analogous complex is one of the best known Fe(III) oxalato complexes, $K_3[Fe(C_2O_4)_3]\cdot 3H_2O$.

The crystal structure of this complex was determined more than half a century ago [3] and refined again more recently [4]. The crystal structures of $K_3[Cr(C_2O_4)_3]\cdot 3H_2O$ [5, 6] and $K_3[Al(C_2O_4)_3]\cdot 3H_2O$ [3, 6] have also been determined, confirming a close structural relation to $K_3[Fe(C_2O_4)_3]\cdot 3H_2O$. An anhydrous form of the complex, $K_3[Fe(C_2O_4)_3]$, has also been obtained and characterized [7].

As part of our mentioned studies of natural and synthetic oxalate compounds [1], it seemed interesting to prepare and characterize other similar complexes showing structural and/or stoichiometric relations to minguzzite. These studies are not only interesting from the chemical and structural point of view, but also from a geochemical perspective, taking into account that the number of known natural oxalates is limited [1] and such studies allow insight into the overall characteristics of these minerals and closely related species.

Notwithstanding, a search on the synthesis and characterization of other salts of $[Fe(C_2O_4)_3]^{3-}$ showed, surprisingly, that apart from the potassium salt only the ammonium salt [8] and three species in the system $K_{3-x}Na_x[Fe(C_2O_4)_3]\cdot yH_2O$ [9] have been described. Therefore, we have attempted to prepare the sodium, rubidium, and cesium salts of the *tris*-oxalatoferrate(III) anion to generate new examples of synthetic compounds closely related to this rare mineral. The results of these studies constitute the main subject of this contribution.

2. Experimental

2.1. Materials and physical measurements

All reagents, of analytical grade, were purchased commercially and used without purification. Sodium, rubidium, and cesium carbonates were products from Aldrich (St. Louis, USA); $FeSO_4\cdot 7H_2O$, NaOH, $H_2C_2O_4\cdot 2H_2O$ and concentrated HNO_3 were from Merck (Darmstadt, Germany). Elemental analyses (C and H) were performed on a Carlo Erba model EA 1108 elemental analyzer. The infrared spectra between 4000 and 400 cm^{-1} were recorded as KBr pellets with a FTIR Bruker EQUINOX-55 spectrophotometer. Room temperature Mössbauer spectra were taken in transmission geometry using a conventional constant acceleration spectrometer of 512 channels with a 5 mCi nominal activity $^{57}CoRh$ source. The spectra were recorded at velocities +7 to −7 mm s^{-1}. The absorber was a powdered sample, whose optimum thickness was calculated with the method of Long *et al*. [10]. Velocity calibration was performed with a 12 μm α-Fe metal foil at room temperature. Isomer shifts (δ) refer to this standard. Mössbauer spectra were numerically analyzed using a computer code that can take into account hyperfine field distributions [11].

2.2. Synthesis of the complexes

Different preparative routes are known for synthesis of $K_3[Fe(C_2O_4)_3]\cdot 3H_2O$. The three most usually employed methodologies can be briefly summarized as follows: (a) H_2O_2 oxidation of Fe(II) oxalate in the presence of oxalic acid and potassium oxalate; (b) direct interaction of $FeCl_3$ and $K_2C_2O_4\cdot H_2O$ solutions; and (c) digestion over a steam bath of a mixture of ferric sulfate, barium oxalate, and $K_2C_2O_4\cdot H_2O$ [1].

In order to optimize the preparation of the three new salts, we have developed a new synthetic strategy based on the combined use of some usual laboratory reagents and consisting in the reaction of freshly precipitated $Fe(OH)_3$ with the hydrogen oxalate of the respective alkaline cation, according to: $Fe(OH)_3 + 3\,M^I(HC_2O_4) + nH_2O \rightarrow M^I_3[Fe(C_2O_4)_3]\cdot nH_2O + 3H_2O$. This procedure gives consistently very high yields (usually above 70%) and generates very pure and well-formed crystalline material.

This general procedure allowed the preparation of crystalline samples of sodium *tris*-oxalatoferrate(III) pentahydrate, $Na_3[Fe(C_2O_4)_3]\cdot 5H_2O$ (**1**), rubidium *tris*-oxalatoferrate(III) trihydrate, $Rb_3[Fe(C_2O_4)_3]\cdot 3H_2O$ (**2**), and cesium *tris*-oxalatoferrate(III) dihydrate, $Cs_3[Fe(C_2O_4)_3]\cdot 2H_2O$ (**3**) as follows:

2.2.1. Synthesis of $Na_3[Fe(C_2O_4)_3]\cdot 5H_2O$ (1)

0.834 g (3 mmol) of $FeSO_4\cdot 7H_2O$ was dissolved in 20 mL of boiling distilled water and oxidized with drops of concentrated HNO_3. The boiling was continued for some further minutes, and then the generated Fe(III) was precipitated as $Fe(OH)_3$ by dropwise addition of 20% NaOH. The precipitate was separated by centrifugation, washed several times with hot water and immediately dissolved in 20 mL of a hot solution containing 1.01 g (9 mmol) of $NaHC_2O_4$ (this solution was prepared by reaction of the necessary amounts of a 1 : 2 mixture of sodium carbonate (0.48 g, 4.5 mmol) and oxalic acid dihydrate (1.14 g, 9 mmol) : $Na_2CO_3 + 2H_2C_2O_4\cdot 2H_2O \rightarrow 2Na(HC_2O_4) + 3H_2O + CO_2$). The obtained solution was allowed to evaporate in air and after a few days small crystals of the sodium salt of the complex were separated and then recrystallized from hot water and air dried (yield = 1.0 g, *ca.* 70%). *Analysis:* Calcd for $C_6H_{10}FeNa_3O_{17}$ (**1**): C, 15.04; H, 2.09. Found: C, 14.97; H, 2.12%.

2.2.2. Synthesis of $Rb_3[Fe(C_2O_4)_3]\cdot 3H_2O$ (2)

The same procedure as outlined above was used employing the following quantities of reagents: 0.834 g (3 mmol) of $FeSO_4\cdot 7H_2O$ and 1.57 g (9 mmol) of $RbHC_2O_4$ (prepared with 1.04 g Rb_2CO_3 and 1.14 g $(COOH)_2\cdot 2H_2O$). The crude product was recrystallized from water and air dried (yield = 1.4 g, *ca.* 75%). *Analysis*: Calcd for $C_6H_6FeRb_3O_{15}$ (**2**): C, 11.42; H, 0.95. Found: C, 11.33; H, 0.92%.

2.2.3. Synthesis of $Cs_3[Fe(C_2O_4)_3]\cdot 2H_2O$ (3)

In this case, the following quantities of reagents were employed: 0.834 g (3 mmol) of $FeSO_4\cdot 7H_2O$ and 2.00 g (9 mmol) of $CsHC_2O_4$ (obtained from 1.47 g Cs_2CO_3 and 1.14 g$(COOH)_2\cdot 2H_2O$). The product was recrystallized from water and air dried (yield = 1.8 g, *ca.* 80%). *Analysis*: Calcd for $C_6H_4Cs_3FeO_{14}$ (**3**): C, 9.54; H, 0.53. Found: 9.50; H, 0.56%.

2.2.4. Synthesis of $K_3[Fe(C_2O_4)_3]\cdot 3H_2O$

We also prepared this well-known salt, which was obtained by reaction of hot solutions of $FeCl_3$ (3.2 g, 20 mmol, in 30 mL H_2O) and $K_2C_2O_4\cdot H_2O$ (12.0 g, 60 mmol, in 30 mL H_2O). The complex, which crystallized after cooling to 0 °C, was recrystallized from minimum amount of warm water and cooled again to 0 °C. Finally, it was collected by filtration, washed with a small volume of ice water and air dried [12]. Anal. Calcd for $C_6H_6FeK_3O_{15}$: C, 15.82; H, 1.32. Found: C, 15.77; H, 1.34%.

2.3. X-ray crystallography and structure solution

The measurements were performed on an Oxford Xcalibur, Eos, Gemini CCD diffractometer with graphite-monochromated MoKα ($\lambda = 0.71073$ Å) radiation. X-ray diffraction intensities were collected (ω scans with ϑ and κ-offsets), integrated and scaled with the CrysAlisPro [13] suite of programs. The unit cell parameters were obtained by least-squares refinement (based on the angular settings for all collected reflections with intensities larger than seven times the standard deviation of measurement errors) using CrysAlisPro. Data were corrected empirically for absorption employing the multi-scan method implemented in CrysAlisPro.

The structures of **1** and **3** were solved by direct methods with SHELXS of the SHELX suite of programs [14] and the molecular model refined by full-matrix least-squares procedure with SHELXL of the same package. In the case of the sodium salt, hydrogens of three of the five crystallization water molecules were located in a difference Fourier map placed on the heavier atoms and refined at their found positions with isotropic displacement parameters and O–H and H···H distances restrained to target values of 0.86(1) and 1.36(1) Å, respectively. The remaining two water molecules showed positional disorder (the oxygen of one was modeled as occupying two split positions with occupancies which added up to

Table 1. Crystal data and structure refinement parameters for **1–3**.

Compound	1	2	3
Empirical formula	$C_6H_{10}FeNa_3O_{17}$	$C_6H_6FeO_{15}Rb_3$	$C_6H_4Cs_3FeO_{14}$
Formula weight	478.96	630.37	754.67
Temperature (K)	297(2)	297(2)	297(2)
Space group	C2/*c*	$P2_1/c$	$P2_1/n$
a (Å)	17.3594(5)	7.9496(6)	8.2716(2)
b (Å)	12.6866(4)	19.975(1)	20.1580(5)
c (Å)	15.1757(5)	10.5115(7)	10.1349(2)
β (°)	100.449(3)	107.247(8)	103.465(2)
V (Å^3)	3286.8(2)	1594.1(2)	1643.43(7)
Z	8	4	4
ρ_{calcd} (g cm^{-3})	1.936	2.627	3.050
Crystal size (mm)	0.299 × 0.155 × 0.089	0.224 × 0.200 × 0.127	0.198 × 0.166 × 0.107
F(0 0 0)	1928	1196	1372
μ (mm^{-1})	1.087	10.125	7.535
θ Range (°)	3.205–26.995	3.371–29.712	2.872–26.998
Reflections collected	7433	7707	8183
Independent reflections	3536	3728	3549
R_{int}	0.0253	0.0401	0.0289
Observed reflections [$I > 2\sigma(I)$)]	2874	2152	2973
Data/restraints/parameters	3536/9/279	3728/0/236	3549/0/217
R_1/wR_2 ($I > 2\sigma(I)$)	0.0375/0.0925	0.0678/0.1674	0.0360/0.0768
R_1/wR_2 (all data)	0.0498/0.1011	0.1225/0.2037	0.0464/0.0833
Goodness-of-fit (GOF) on F^2	1.041	1.025	1.063
Δρ min/max (e Å^{-3})	0.714/−0.496	1.819/−3.355	2.228/−1.925

one) and therefore their hydrogens could not be determined reliably and were not included in the final molecular model. The water molecules of the cesium salt also showed positional disorder and therefore their hydrogens could not be determined reliably for their inclusion in the final molecular model.

The same space group and very similar unit cell constants strongly suggested that the rubidium salt is isotypic to the previously reported potassium salt, $K_3[Fe(C_2O_4)_3]\cdot 3H_2O$ [5]. In fact, a least squares refinement of an initial molecular model based on the published structure against the rubidium diffraction data-set led to smooth convergence of the structure parameters. An also isostructural K/Na solid solution, $K_{2.9}Na_{0.1}[Fe(C_2O_4)_3]\cdot 3H_2O$ has been reported [9a]. $Rb_3[Fe(C_2O_4)_3]\cdot 3H_2O$ showed disordered water molecules and one was modeled in terms of two split oxygen positions and refined while keeping the sum of their occupancy equal to one. As a consequence of disorder, the water hydrogens could not be determined reliably and therefore they were not included in the final molecular model.

Crystal data, data collection procedure, and refinement results for **1–3** are summarized in table 1.

3. Results and discussion

3.1. Description of the structures

The $[Fe(C_2O_4)_3]^{3-}$ anion in all three alkali salt crystals shows a distorted FeO_6 octahedral geometry. The Fe(III) ion is coordinated to three bidentate oxalate molecules through the oxygens of their opposite carboxylate groups in a propeller-like conformation as shown in the ORTEP [15] drawing (figure 1) for the sodium salt. Table 2 compares bond distances and angles around iron for the three salts. Despite the different crystal environments, $[Fe(C_2O_4)_3]^{3-}$ shows very nearly the same molecular structure and metric in all salts.

For the better refined sodium-containing salt, Fe–O distances are 1.992(2)–2.021(2) Å and *cis* and *trans* O–Fe–O angles are 80.20(8)–111.49(9)° and 164.60(8)–166.75(8)°, respectively. All three oxalate ligands are nearly planar (*rms* deviation of atoms from the best least-squares plane less than 0.053 Å) with the iron close to the intersection of the oxalate planes. The oxalate C–O distances for coordinated-to-iron oxygens are 1.274(3)–1.286(3) Å, compatible with a formal single bond. The C–O lengths for uncoordinated oxygens are 1.220(3)–1.224(3) Å and correspond to a formal double bond character for

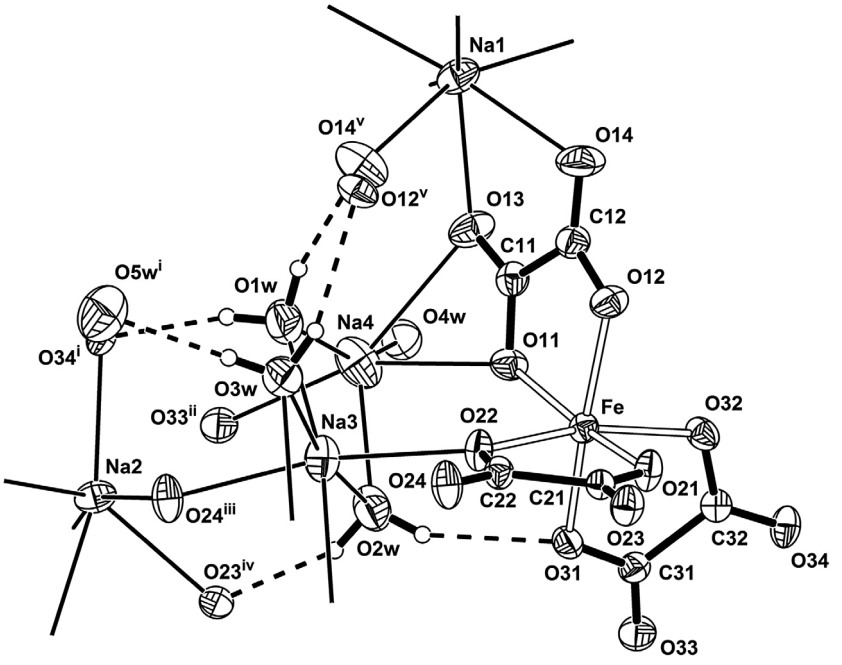

Figure 1. Plot of $Na_3[Fe(C_2O_4)_3]\cdot 5H_2O$ (**1**) crystal showing the labeling of the atoms and their displacement ellipsoids (except disordered O4w) at 50% probability. Fe-oxalate and Na–oxygen bonds are indicated by open and thin lines, respectively, and H-bonds by dashed lines. Symmetry operations: (i) $-½ + x, ½ - y, -½ + z$; (ii) $½ - x, ½ - y, -z$; (iii) $-x, -y, -z$; (iv) $x, -y, -½ + z$; (v) $-x, y, ½ - z$.

Table 2. Bond lengths (Å) and angles (°) around Fe(III) in **1–3**.

Compound **1**		Compound **2**		Compound **3**	
Fe–O(11)	1.992(2)	Fe–O(11)	2.007(6)	Fe–O(11)	2.014(4)
Fe–O(12)	2.010(2)	Fe–O(12)	2.005(6)	Fe–O(12)	2.004(4)
Fe–O(21)	2.003(2)	Fe–O(21)	2.021(6)	Fe–O(21)	1.988(4)
Fe–O(22)	2.021(2)	Fe–O(22)	1.984(6)	Fe–O(22)	2.015(4)
Fe–O(31)	1.999(2)	Fe–O(31)	2.028(6)	Fe–O(31)	2.003(4)
Fe–O(32)	2.021(2)	Fe–O(32)	1.988(6)	Fe–O(32)	2.014(4)
O(11)FeO(12)	80.53(8)	O(11)FeO(12)	80.5(3)	O(11)FeO(12)	80.1(2)
O(21)FeO(22)	80.20(8)	O(21)FeO(22)	80.4(2)	O(21)FeO(22)	80.2(2)
O(31)FeO(32)	80.47(7)	O(31)FeO(32)	80.4(2)	O(31)FeO(32)	80.3(2)
O(11)FeO(21)	166.75(8)	O(11)FeO(21)	164.0(3)	O(11)FeO(21)	164.0(2)
O(11)FeO(22)	92.72(8)	O(11)FeO(22)	89.4(3)	O(11)FeO(22)	92.6(2)
O(11)FeO(31)	90.81(8)	O(11)FeO(31)	86.8(2)	O(11)FeO(31)	88.2(2)
O(11)FeO(32)	101.49(9)	O(11)FeO(32)	101.7(3)	O(11)FeO(32)	100.4(2)
O(12)FeO(21)	89.34(8)	O(12)FeO(21)	89.1(2)	O(12)FeO(21)	87.3(2)
O(12)FeO(22)	98.05(8)	O(12)FeO(22)	100.4(3)	O(12)FeO(22)	101.4(2)
O(12)FeO(31)	165.81(9)	O(12)FeO(31)	162.8(3)	O(12)FeO(31)	163.7(2)
O(12)FeO(32)	90.20(8)	O(12)FeO(32)	90.7(3)	O(12)FeO(32)	90.7(2)
O(21)FeO(31)	100.73(9)	O(21)FeO(31)	105.5(3)	O(21)FeO(31)	106.1(2)
O(21)FeO(32)	86.95(8)	O(21)FeO(32)	90.6(2)	O(21)FeO(32)	89.5(2)
O(22)FeO(31)	93.54(8)	O(22)FeO(31)	91.0(2)	O(22)FeO(31)	90.3(2)
O(22)FeO(32)	164.60(8)	O(22)FeO(32)	165.5(3)	O(22)FeO(32)	163.6(2)

these bonds. Curiously, when compared with $Tl_2(C_2O_4)(C_2O_4H_2)$ [16], where both oxalate ($C_2O_4^{2-}$) and neutral oxalic acid ($C_2O_4H_2$) are present, the above C–O bond distances for $[Fe(C_2O_4)_3]^{3-}$ are closer to the corresponding bond lengths of $C_2O_4H_2$ [d(C=O) = 1.21(1) Å, d(C–OH) = 1.29(1) Å] than to the oxalate ion, where C-O bond lengths are 1.24(1) and 1.28(1) Å, the longer one corresponding to the oxygen at

the shortest contact [2.757(7) Å] with thallium(I). This can be rationalized considering that the electron withdrawing capacity of both protons in $C_2O_4H_2$ is replaced by Fe(III) ion upon coordination of $C_2O_4^{2-}$ ions to the metal, without appreciable changes in the ligand bonding structure.

These structural data are in agreement with the corresponding ones of the rubidium and cesium salts reported here and also with the data published for the potassium analog [5].

In **1** (see figure 1), there are four independent sodium ions, two of them on crystallographic twofold axes and (within a coordination sphere of 2.7 Å radius) in a distorted sixfold polyhedral environment of carboxylate oxygens of neighboring $[Fe(C_2O_4)_3]^{3-}$ complexes [Na–O short contacts are 2.399(2)–2.570(2) Å]. The other two sodium ions (in general positions) are also in distorted octahedral environments that include carboxylate oxygens [Na–O distances in the range 2.403(2)–2.702(2) Å] and water molecules [Na–Ow distances in the range 2.235(2)–2.454(2) Å].

Compound **2** is isotypic to $K_3[Fe(C_2O_4)_3]\cdot 3H_2O$ salt [5] and therefore the environment of oxygens around each of the three distinct rubidium ions in the former lattice are closely related to the potassium ones in the latter crystal, with an expected small swelling of average Rb–O contact distances as compared with K–O distances due to the slightly larger ionic radius of Rb^+ (1.51 Å) as compared with K^+ ion (1.38 Å). As coordination around potassium ions in $K_3[Fe(C_2O_4)_3]\cdot 3H_2O$ has been fully detailed [5], we shall not discuss this subject any further here.

Within a coordination sphere of up to 3.4 Å radius, the three independent cesium ions in **3** are, respectively, in a fivefold distorted polyhedral environment [Cs–O(carb) distances in the 3.087(4)–3.324(4) Å range and d(Cs–Ow) = 3.008(7) Å], a distorted octahedron [Cs–O(carb) in the 3.050(4)–3.287(5) Å range], and a sevenfold distorted polyhedron [Cs–O(carb) in the 3.071(4)–3.224(5) Å range and d(Cs–Ow) = 3.177(7) Å].

3.2. Infrared spectra

To extend knowledge of the general physicochemical properties of the new salts of $[Fe(C_2O_4)_3]^{3-}$ we have analyzed their infrared spectra. The spectra of these complexes are similar in general structure, band patterns and intensity distribution, and also show close analogies to that of the well-known IR spectrum of $K_3[Fe(C_2O_4)_3]\cdot 3H_2O$ [17], clearly suggesting that they are dominated by the vibrations of the $[Fe(C_2O_4)_3]^{3-}$ skeleton.

The obtained spectra have been analyzed on the basis of the classic papers of Fujita *et al.* [17, 18] on the vibrational behavior of $K_2[M^{II}(C_2O_4)_2]\cdot nH_2O$ and $K_3[M^{III}(C_2O_4)_3]\cdot 3H_2O$ (cf also [19]) and also using information derived from our previous studies on metallic oxalato complexes [1].

As the $Fe(C_2O_4)_3]^{3-}$ skeleton of the investigated complexes possess approximately D_3-symmetry, its 51 internal vibration modes are distributed as follows:

$$\Gamma_{vib} = 8A_1 + 9A_2 + 17E$$

where the A_1 species are Raman active, the A_2 species infrared active, and the E species are active in both the Raman and the infrared [20]. Therefore, a significant number of IR bands can be expected in the measured spectra.

As examples for the measured spectra, FTIR spectra of **1** and **3** are shown in figure 2 and the assignments proposed for them, along with the ones for **2** and $K_3[Fe(C_2O_4)_3]\cdot 3H_2O$, are presented in table 3 and briefly discussed as follows:

The characteristic O–H stretching vibrations of water molecules are seen, as usual, as a relatively strong and broad band in all spectra. The band broadening and the appearance of some additional peaks are surely related to the presence of different kinds of hydrogen bonds involving these water molecules. From the spectroscopic point of view these hydrogen bridges classify as medium strength ones [21]. The deformational mode of H_2O molecules are overlapped by the strong IR bands located above 1600 cm^{-1}. One of the expected $\rho(H_2O)$ motions was also tentatively assigned in the spectral region around 580 cm^{-1}. Additional bands of this type may also be located at 450–480 cm^{-1} as suggested from data available for other aqua complexes [19].

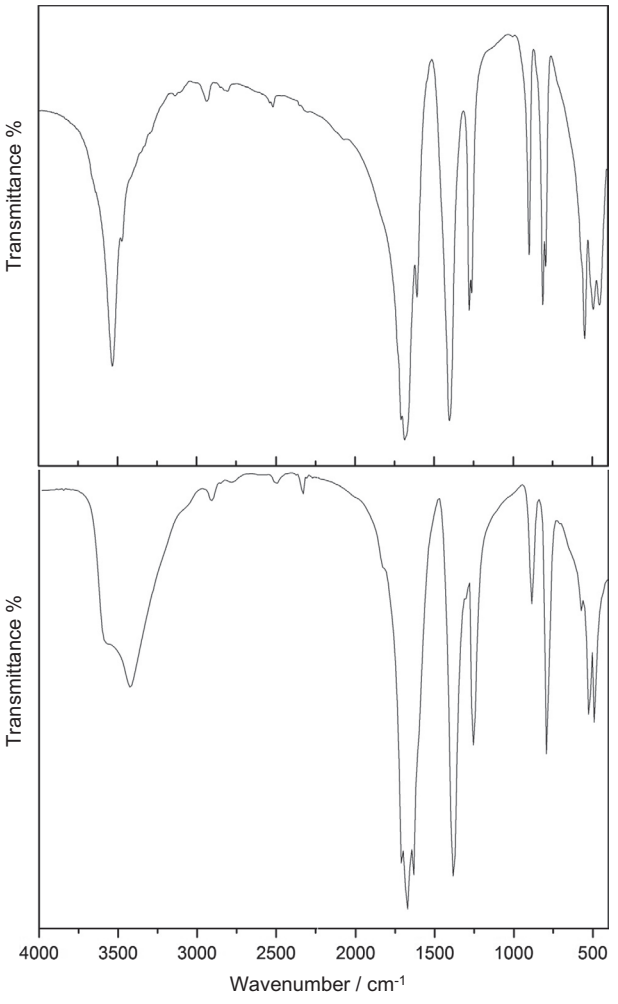

Figure 2. FTIR spectra of $Na_3[Fe(C_2O_4)_3]\cdot 5H_2O$ (**1**) (above) and $Cs_3[Fe(C_2O_4)_3]\cdot 2H_2O$ (**3**) (below) in the spectral range from 4000 to 400 cm^{-1}.

Table 3. Assignment of vibration modes in FTIR spectra of the $M^I_3[Fe(C_2O_4]\cdot nH_2O$ salts.

$M^I = Na^+$ (**1**)	$M^I = K^+$	$M^I = Rb^+$ (**2**)	$M^I = Cs^+$ (**3**)	Assignment
3533 s, 3472 w	3584 m, 3426 s	3595 m, 3438 s	3594 m, 3433 s	ν(OH) (H_2O)
1731 w, 1708 vs	1716 vs	1715 vs	1714 s	ν_{as}(C=O)
1687 vs, 1670 w	1698 w, 1682 vs	1684 vs	1682 vs	ν_{as}(C=O)
1608 m	1660 w, 1644 vs	1660 sh	1644 s	ν_{as}(C=O)
1405 vs	1391 vs	1399 vs	1399 vs	ν_s(C=O)+ν(CC)
1278 vs, 1264 s	1273 s, 1256 m	1273 vs, 1256 m	1270 s, 1256 w	ν_s(C=O)+δ(O–C=O)
898 s	892 m	892 m	892 m	ν_s(C=O)+δ(O–C=O)
812 vs, 793 s	805 s, 792 sh	805 vs, 790 sh	804 vs, 790 sh	δ(O–C=O)
571 sh	586 w	582 w	583 w	ρ(H_2O)(?)
547 s	532 m	532 s	531 m	ν(MO) + ν(CC)
494 m, 455 m	503 m	502 s	500 m, 449 m	δ(O–C=O) + δ_{ring}

Note: vs, very strong; s, strong; m, medium; w, weak; sh, shoulder.

In agreement with its isotypic nature, the K/Rb pair present very similar spectral patterns, although all the splittings are better defined in the case of the $K_3[Fe(C_2O_4)_3]\cdot 3H_2O$ complex.

The antisymmetric C=O stretching vibration generates, in all cases, three strong IR bands, which in the case of the sodium and potassium salts present some additional weak splittings.

The corresponding symmetric C=O mode, coupled with the *v*(CC) vibration, is detected as a very strong and well-defined IR band, accompanied by a well-resolved doublet at lower energies.

As derived from theoretical studies [17, 18], and as a consequence of the low symmetry of the chelate ring and the fact that the force constants for *v*(C–O), *v*(C–C), and *v*(M–O) vibrations are of similar magnitude, bands related to the symmetric C=O stretching modes are strongly coupled with other vibrations. Notwithstanding, two components on this symmetric C=O mode, coupled with the *v*(C–C) vibration, can be assigned with confidence. They are always seen as a very strong and well-defined IR band, accompanied by a well-resolved doublet at somewhat lower energies.

One of the *v*(Fe–O) vibrations, surely coupled with other motions, has been tentatively assigned to occur at 531–547 cm^{-1}, by comparison with the spectra of other *tris*-oxalatometal complexes [17, 19].

3.3. Mössbauer spectra

Figure 3 displays Mössbauer spectra taken at 298 K of the complex salts. The determined parameters are shown in table 4. All spectra exhibit a very broad central peak of parameters typical of Fe(III) in a regular environment of high symmetry. However, it is not common to observe a line-broadening of

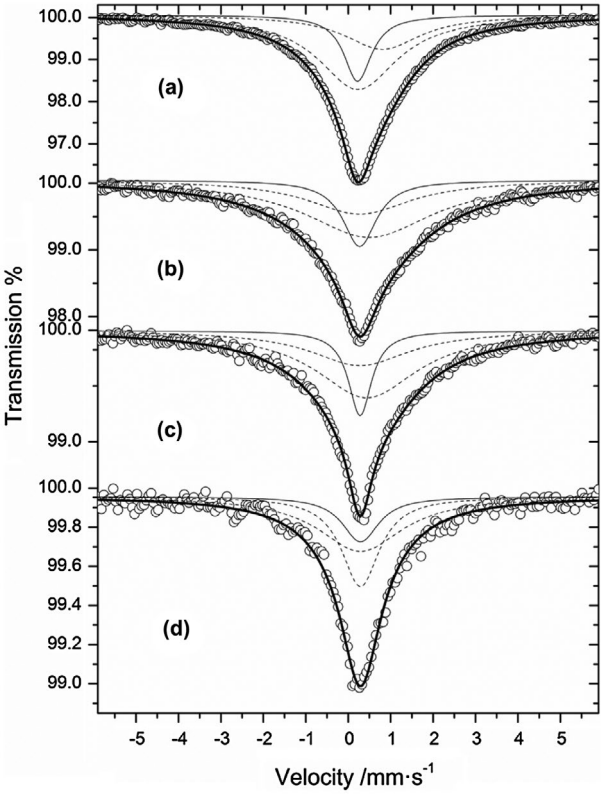

Figure 3. Mössbauer spectra at 298 K for the compounds: (a) $Na_3[Fe(C_2O_4)_3]\cdot 5H_2O$ (**1**), (b) $K_3[Fe(C_2O_4)_3]\cdot 3H_2O$, (c) $Rb_3[Fe(C_2O_4)_3]\cdot 3H_2O$ (**2**) and (d) $Cs_3[Fe(C_2O_4)_3]\cdot 2H_2O$ (**3**). The open circles are the experimental data. The thick solid lines symbolize the fittings performed according to the way described in the text. The thin solid lines are the central narrower components. The dashed lines display peaks originating in the spin–spin relaxation taking place in the compounds, fitted according to the model [24].

Table 4. Hyperfine parameters obtained after fitting the 298 K Mössbauer spectra of the investigated oxalato complexes to three Lorentzian-shaped singlets. The parameters belonging to the central narrower lines carry the information reflecting the possible influence of the alkaline metals on the hyperfine field of Fe(III). Isomer shifts (δ) are referred to the center shift of a α-Fe foil, at room temperature. Parameters of sites 2 and 3 are related to the relaxation mechanism that has not been studied in this work.

	δ (mm s^{-1})	Γ (mm s^{-1})	Spectral area %
$Na_3[Fe(C_2O_4)_3]\cdot 5H_2O$			
Site 1	0.23 ± 0.02	0.42 ± 0.04	18 ± 6
Site 2	0.23 ± 0.10	1.13 ± 0.08	57 ± 20
Site 3	0.81 ± 0.20	1.08 ± 0.81	25 ± 26
$K_3[Fe(C_2O_4)_3]\cdot 3H_2O$			
Site 1	0.27 ± 0.01	0.48 ± 0.09	17 ± 4
Site 2	0.27 ± 0.10	1.43 ± 0.08	27 ± 15
Site 3	0.49 ± 0.35	1.83 ± 0.33	56 ± 18
$Rb_3[Fe(C_2O_4)_3]\cdot 3H_2O$			
Site 1	0.28 ± 0.01	0.33 ± 0.05	16 ± 4
Site 2	0.28 ± 0.10	0.48 ± 0.09	28 ± 12
Site 3	0.44 ± 0.20	1.45 ± 0.81	56 ± 21
$Cs_3[Fe(C_2O_4)_3]\cdot 2H_2O$			
Site 1	0.29 ± 0.02	0.34 ± 0.04	17 ± 6
Site 2	0.29 ± 0.10	1.2 ± 0.8	35 ± 25
Site 3	0.29 ± 0.20	2.4 ± 1.9	48 ± 46

about 10 times the natural line-width. This result indicates that in these compounds there is relaxation taking place.

Previous works on the Mössbauer spectrum of K_3 $[Fe(C_2O_4)_3]\cdot 3H_2O$ can be found only in a few references [1]. In particular, in one that studied the thermal decomposition of the compound by heating it to 700 °C [22], the broad single line displayed at 298 K in the Mössbauer spectra of a sample heated to 270 °C was fitted to a Lorentzian singlet of isomer shift 0.31 ± 0.03 mm s^{-1} and a line-width of 2.00 mm s^{-1}. Because the goal of that work dealt with identification of the thermal decomposition products, no mention is made about the relaxation-broadened line of the spectrum at room temperature.

The broadening issue had been studied previously by Barb *et al*. [23] and ascribed to electronic spin relaxation of the Fe(III) ions in the $^6S_{5/2}$ ground state. It is well known that Mössbauer relaxation spectra typically display complex shapes. Usually, this depends on the relaxation time compared to the Larmor precession time, ranging from complete split spectra at the slow limit to totally collapsed spectra at the fast one. At intermediate relaxation times, several models can be found in the literature to fit the spectra.

According to Barb *et al*. [23], spin–spin relaxation occurs when Fe(III) ions are located at distances larger than 5 Å, which is fulfilled in our case. Indeed, irrespective of the crystalline structure, the shortest Fe–Fe distances obtained by X-ray diffraction analyses give for the Na, K, Rb, and Cs compounds: 6.65, 7.02, 7.11, and 7.40 Å, respectively.

To simulate the broadened lineshape, Barb *et al*. [23] used the models by Afanas'ev and Gorobchenko [24] and Blume and Tjon [25]. The Afanas'ev and Gorobchenko model gives a better fit [23] and uses a simple sum of three Lorentzians to simulate the broad line.

Our goal at this time is not centered at the detailed description of the electronic spin relaxation undergone by Fe(III) ions, but rather to assess the influence of the nature of the alkaline metals on the hyperfine parameters of the compounds. Therefore, as in Ref. [23], we decided to fit the spectra with a simple model that utilized three Lorentzian-shaped lines. Because the quadrupole splitting is almost negligible compared to the line-width, we have used singlets, which should yield roughly similar results. The relative population of each site derived from the current results agrees broadly with the Afanas'ev and Gorobchenko model [24]. To account for the specific details of relaxation mechanism of some spectra, some lines display a different isomer shift than the other two. This might also be the case of the spectra of reference [23] if those spectra had higher statistics.

These fittings by no means are unique and the results obtained do not mean that the model is the only one that can achieve such a good χ^2-value. Instead, it should be understood that if it is assumed that the broadening occurs because of a spin–spin relaxation at play in the systems, the reasonable fittings attained with the model [24] do not deny such assumption.

For our purposes, the narrower central line of the spectrum at room temperature carries information relevant to the influence of the alkaline metals on the Mössbauer spectra. The relaxation components are evidence of a spin–spin relaxation whose detailed mechanism would require taking careful measurements at different temperatures to improve the approximate model [24].

For all the alkaline metal oxalates studied, the isomer shifts lie within the experimental uncertainties and therefore the influence of the metals on the spectra are essentially not distinguishable from one another. However, a slight trend toward an increasing isomer shift and therefore to a lower electron density at Fe(III) might be inferred from the experimental results, indicating that the larger radii of the alkaline metal ions lessen slightly the electron density at the Fe(III) sites.

Since the central line is also affected by relaxation, we cannot unambiguously distinguish a possible contribution from a quadrupole splitting to the line broadening for the different alkaline cations along the series that might be originated in distortions of the electronic structure of the coordination polyhedra of Fe(III) ions. However, the very similar shapes of the four spectra indicate that it does not seem to be significant.

In contrast to the statement that the observation of the relaxation effects in hydrated crystals are easier to observe [23], it is clear from the results of Ladrière [22] that almost the same line broadening is experienced by the central Mössbauer line when the crystal water does not exist in the compound after heat treatment to the potassium salt of the complex.

4. Conclusion

In order to find new oxalato complexes, stoichiometrically related to the rare mineral minguzzite ($K_3[Fe(C_2O_4)_3]\cdot 3H_2O$), the Na^+, Rb^+, and Cs^+ salts of the $[Fe(C_2O_4)_3]^{3-}$ were prepared using a new general synthetic procedure developed for these preparations. The crystal structures of these salts, ($Na_3[Fe(C_2O_4]\cdot 5H_2O$, $Rb_3[Fe(C_2O_4]\cdot 3H_2O$, and $Cs_3[Fe(C_2O_4]\cdot 2H_2O$), were determined by single-crystal X-ray diffractometry. The Rb-salt is isotypic to $K_3[Fe(C_2O_4]\cdot 3H_2O$, prepared for comparative purposes. The FTIR spectra of the four salts were discussed. Analysis of their ^{57}Fe-Mössbauer spectra confirmed the presence of a relaxation phenomenon. A slight increase of the isomer shift with increasing cationic radii is observed, suggesting a slight decrease of electron density at Fe(III) with increasing cationic size.

Supplementary material

Complete crystallographic data for **1–3** have been deposited with the Cambridge Crystallographic Data Center, CCDC 1472715 (**1**), 1472716 (**2**), 1472717 (**3**). These data can be obtained free of charge from the Cambridge Crystallographic Data Center via www.ccdc.cam.ac.uk/data_request/cif.

Acknowledgements

OEP, GAE, RCM, and ACGB are Research Fellows of CONICET.

Disclosure statement

No potential conflict of interest was reported by the authors.

Funding

This work was supported by the Universidad Nacional de La Plata and by ANPCyT [grant number PME06 2804], [grant number PICT06 2315] of Argentina.

References

[1] E.J. Baran. *J. Coord. Chem.*, **67**, 3734 (2014).
[2] T. Echigo, M. Kimata. *Can. Mineral.*, **48**, 1329 (2010).
[3] P. Herpin. *Soç. Franc. Minèral. Cristallogr.*, **81**, 245 (1958).
[4] P.C. Junk. *J. Coord. Chem.*, **58**, 355 (2005).
[5] J. Van Niekerk, F.R.L. Schoening. *Acta Crystallogr. A*, **5**, 196 (1952).
[6] D. Taylor. *Aust. J. Chem.*, **31**, 1455 (1978).
[7] A. Saritha, B. Raju, M. Ramachary, P. Raghavaiah, K.A. Hussain. *Physica B*, **407**, 4208 (2012).
[8] P.E.H. Merrachi, F. Chassagneux, B.F. Mentzen. *Powder Diffr.*, **3**, 96 (1988).
[9] (a) R. Wartchow. *Z. Kristallogr.-New Cryst. Struct.*, **212**, 83 (1997); (b) S. Henneicke, R. Wartchow. *Z. Kristallogr.*, **212**, 56 (1997); (c) R. Wartchow. *Z. Kristallogr.*, **212**, 57 (1997).
[10] G.J. Long, T.E. Cranshaw, G. Longworth. *Mössbauer Effect Refer. Data*, **6**, 42 (1983).
[11] K. Lagarec, D.G. Rancourt. *Mössbauer Spectral Analysis Software. Recoil, Version 1.05*, Department of Physics, University of Ottawa, Ottawa (1998).
[12] R.C. Johnson. *J. Chem. Educ.*, **47**, 702 (1970).
[13] CrysAlisPro, Oxford Diffraction Ltd., version 1.171.37.31 (release 14.01.2014 CrysAlis171.NET).
[14] G.M. Sheldrick. *Acta Crystallogr. A*, **64**, 112 (2008).
[15] L.J. Farrugia. *J. Appl. Crystallogr.*, **30**, 565 (1997).
[16] O.E. Piro, G.A. Echeverria, A.C. Gonzalez-Baró, E.J. Baran. *Z. Naturforsch.*, **70b**, 249 (2015).
[17] J. Fujita, A.E. Martell, K. Nakamoto. *J. Chem. Phys.*, **36**, 324 (1962).
[18] J. Fujita, A.E. Martell, K. Nakamoto. *J. Chem. Phys.*, **36**, 331 (1962).
[19] K. Nakamoto. *Infrared and Raman Spectra of Inorganic and Coordination Compounds*, 6th Edn., Wiley, New York (2009).
[20] H.G.M. Edwards, N.C. Russell. *J. Mol. Struct.*, **443**, 223 (1998).
[21] H. Siebert. *Anwendungen der Schwingunsspektroskopie in der Anorganischen Chemie*, Springer, Berlin (1966).
[22] J. Ladriere. *Hyperfine Interact.*, **70**, 1095 (1992).
[23] D. Barb, L. Diamandescu, D. Tarabasan. *J. Phys. Colloques*, **37**, 113 (1976).
[24] A.M. Afanas'ev, V.D. Gorobchenko. *Zh. Eksp. Teor. Fiz.*, **67**, 2246 (1975).
[25] M. Blume, J.A. Tjon. *Phys. Rev.*, **165**, 446 (1968).